Arabian Journal for Science and Engineering (2023) 48:8417–8430
https://doi.org/10.1007/s13369-022-06853-y

RESEARCH ARTICLE-CHEMICAL ENGINEERING

Pattern, Forms and Bibliometric Analysis for Systematic Study of Silica-Supported Heterogeneous Solar Photocatalyst for Lannate Insecticide Abatement from Aqueous Stream

Maha A. Tony[1]

Received: 20 January 2022 / Accepted: 29 March 2022 / Published online: 6 June 2022

Abstract
Agro-industrial streams with high toxic loadings must undergo for treatment prior to final disposal. Thus, the current investigation aimed to apply cheap and naturally available materials to explore sustainable heterogeneous solar/Fenton reaction for insecticide abatement form waste streams. Iron was collected from the wastewater stream after coal industry. The sand pellets were used as iron support material which acts as a heterogeneous solar photo-catalyst like modified Fenton reaction. The prepared catalysts were characterized using X-ray diffraction (XRD) and scanning electron microscope (SEM) for characterization. System parameters variables were studied using the modified catalysts. Although the acidic pH showed maximal removal efficiency, the catalyst could also work at a wide pH range with a reduced activity. The optimum conditions of the newly synthesized modified Fenton composite showed 103, 45 mg/L for H_2O_2 and catalyst, respectively, at pH 2.8 within 90 min under solar irradiation for maximal Lannate oxidation reached to 98%. Moreover, the increase in Lannate concentration loading results in a reduction in the removal efficiency from 98 to 96% when the Lannate loading increased from 10 to 50 ppm, although further increase of Lannate (100 ppm) results in only 2% removal. Also, temperature effect was displayed and the high temperature range was unfavorable. The kinetics of Lannate removal was dependent on operation temperature and following the first-order kinetic model. The thermodynamic parameters values settled the system is non-spontaneous in nature, proceeds in endothermic circumstances and working in a low energy barrier (34.54 kJ mol^{-1}). Recyclability confirms the sustainability of the catalyst, and the third cycle catalytic use attained 28% Lannate removal.

Keywords Fenton's reaction · Heterogeneous catalyst · Solar photocatalyst · Parabolic collector · Wastewater remediation

1 Introduction

Recently, there is an ever-increasing alarm associated with the emerging pollutants (EPs) streams augmented wastewater discharge from industrial effluents and human consumption. Insecticides that are categorized as EPs have attained a significant attention of scientists and academia due to their negative potential impact on both aquatic system and human health. The presence of Lannate insecticide, which is signified as a restricted-use insecticide, was firstly introduced by E.I. du Pont de Nemours in 1968 [1]. It could present in sewage as a continuous discharge from agriculture land use by human activities or may be from manufacturing plants, which in this case is at substantially higher concentrations [2, 3]. However, Lannate is categorized as one of the most consumed insecticides in many countries, especially in Egypt [4]. It is applied into a broad variety of agricultural crops in order to control a wide spectrum of arthropods. Lannate is formulated as a soluble concentrate and water-soluble powder insecticide with active ingredients among the other commercial formulations [5]. However, it is categorized as toxic to human, mammals and aquatic texture according to US EPA regulations [6]. Thus, treating the effluents contaminated with such insecticide is urgent to satisfy the environmental regulations.

Generally, conventional remediation techniques are inefficient in treatment of such toxic contaminants since they might transfer the pollutants from one to another phase, expensive or resulting in secondary pollutants contaminants.

✉ Maha A. Tony
dr.maha.tony@gmail.com

[1] Advanced Materials/Solar Energy and Environmental Sustainability (AMSEES) Laboratory, Basic Engineering Science Department, Faculty of Engineering, Menoufia University, Shebin El-Kom, Egypt

Subsequently, advanced oxidation processes (AOPs) arose the researchers attention because they possess in situ remediation in a cost-efficient way [7]. Photo-Fenton reaction is one of the AOPs which are superior treatment process that is in the requirement of H_2O_2, iron salts and mostly acidic pH range that leads to the formation of the powerful hydroxyl radicals groups that are the main responsible of remediation. Fenton is simple to operate, efficient and moderately applicable [7, 8]. However, Photo-Fenton's reaction still possesses some limitations including the impact of the sludge by-product formation after the reaction, limited acidic pH conditions [9] and thereby acidic pH range to the final reclaimed wastewater that require further treatment, and finally, the ultraviolet source to conduct the photo-Fenton process is costly and added value to the process cost. Thus, searching for alternatives to overcome such drawbacks is a suggestive topic [10, 11].

In pursuit of overcoming such Fenton's limitations, numerous modifications are developed. The photo-Fenton process was developed by introducing a solar light as a cheap natural UV source to the Fenton process which helps in H_2O_2 molecules dissociation for easy reactivity [12]. Also, it assists in converting Fe^{3+} into Fe^{2+} after reaction. The process helps in improving the performances and kinetics of the process since it decreases the reagents demand. However, solar/photo-Fenton does not address the other process boundaries, especially the operational acidic pH and the final sludge in the effluent [13].

Another key modification to overcome the sludge problem and eliminating the limitations of low pH, use of heterogeneous Fenton processes that entails embedment of the ferrous catalyst is a carrier on supporting material [14]. The support material helps in slowing the catalyst release into the solution. Such method limits the catalyst supply in the effluent; thereby, minimal sludge and metal ions are formed in the final reclaimed water. Moreover, the extreme low pH conditions could be evaded through immobilizing the acid on the carrier support. Additionally, to add to the advantages of the supported heterogeneous Fenton reaction, the catalyst material could be easily separated, recovered and reused for a sustainable application [15]. Various materials are introduced as a possible supported carrier materials for heterogeneous Fenton reaction system. Such carriers include activated carbon, clay, synthetic zeolite and silica [16–21]. However, the principal limitations of the suggested groups are either low efficiency or the high costs. Activated carbon and zeolite are the most studied materials; silica is the most cost-efficient carrier among the studied groups.

The essential need of highly aggressive chemicals in effluent treatments motivates the current work into seeking for a reusable catalyst with an environmentally benign material. Herein, in this regard, the current investigation is seeking to develop an effective heterogeneous photo-Fenton oxidation system that will stunned the drawback of the classical Fenton's reaction. Such catalyst is a novel recyclable solar/Fenton catalyst through extending the operating pH range, reducing the final sludge formation, minimizing the remnant iron ions in the reclaimed effluent. Furthermore, the catalyst is categorized as a cost-efficient since it that could be recoverable after treatment for further use. Moreover, such catalyst could overcome the sludge formed after the Fenton's reaction. The investigation tested several oxidation parameters for the modified iron-coated silica carrier to develop a cheap and more effective carrier material for heterogeneous Fenton process. Additionally, the system kinetics and thermodynamic parameters are investigated at different temperature effects.

2 Bibliometric Analysis

Bibliometric analysis is used as a valuable tool for relevant research literature analysis for selected topic. Such technique could be applied and identified to link key aspects of a certain subject. The achieved bibliometric mapping signifies the highest cited articles published in literature and the investigation of relationships between the terms attained. As such, a search at the database of the "Web of Science" via the keywords of "Pesticide wastewater AND advanced oxidation processes" was performed and 308 publications, in scientific journals from the year 2000 to August of 2021. In spite of the relatively limited papers in the last 20 years, Fig. 1 shows a profile of the current studies related to the wastewater containing pesticide oxidation through advanced oxidation processes. The increased number of research articles helps in

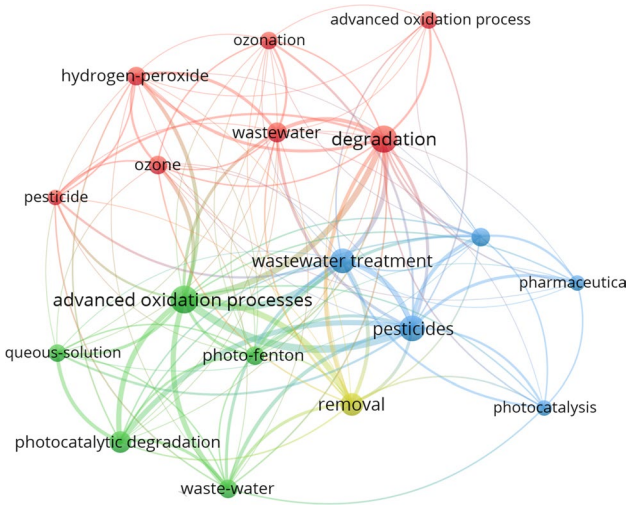

Fig. 1 Bibliometric network mapping generated in VOSviewer from the search terms of wastewater containing pesticide and advanced oxidation processes

further development of wastewater reclaiming using AOPs for high levels for final sustainable disposal. The keywords were analyzed through the VOSviewer software to analyze the articles conducting such studies. The bibliometric network mapping generated in VOSviewer based on 308 papers from the search terms is displayed in Fig. 1. The clusters represent hotspot. From such map, a considerable attention could be paid as the photo-Fenton has been intensively identified among the other AOPs.

3 Box–Behnken Design (BBD) Model

Response surface methodology (RSM) is introduced as a statistical technique and applied for attaining the optimum experimental values of the operating parameters [22]. Box–Behnken Design (BBD) is chosen as a statistical tool based on a multivariate nonlinear model for optimizing the response surface that influencing various variables as well as categorizing the correlation between the controllable variables and the evaluated response. RSM is signified as an effective tool for optimizing the interacting variables in the Fenton process in order to optimize pollutant oxidation since Fenton reaction is a multivariable dependent process. In the present investigation, the most influencing variables in the Fenton's reaction were chosen to investigate their influence in the Lannate removal (as a response), i.e., H_2O_2, silica-supported iron catalyst concentrations and pH were selected to explore their effect on Lannate concentration removal (γ) efficiency from aqueous stream. The levels of the experimental variables were determined according to the preliminary study by the author (results are not shown). Three levels were chosen for each of the three variables: H_2O_2 (τ_1), catalyst (τ_2) and pH (τ_3) as displayed in Table 1 in their uncoded and coded values.

Table 2 tabulates the full factorial BBD experimental design that fits the second-order polynomial model. Commonly, the optimization technique includes main steps: the first step is dealing with conducting the statistically designed experiments (Table 2), followed by the estimation of the coefficients in a mathematical model, and lastly the predicted response is attained and the adequacy of the model is checked. Developing of an empirical model that correlates the response of the Lannate removal process is attained that is based on second-order quadratic model as given by Eq. (1) to interact the interaction variables.

$$\gamma = \beta_o + \sum \beta_i \Gamma_i + \sum \beta_{ii} \Gamma_i^2 + \sum \beta_{ij} \Gamma_i \Gamma_j \quad (1)$$

where $\boldsymbol{\gamma}$ is the Lannate concentration removal response; β_o, β_i, β_{ii} and β_{ij} are the model coefficient of the linear effect and double interactions; $\boldsymbol{\Gamma_i}$ and $\boldsymbol{\Gamma_i^2}$ are the independent parameters.

Table 1 Boundaries of the experimental domain and spacing of levels expressed in coded and natural units for Lannate remediation through dual oxidation system

Variable	Symbols		Range and levels		
	Natural	Coded	− 1	0	1
H_2O_2 (mg/L)	τ_1	Γ_1	50	100	150
Silica-supported Fe (mg/L)	τ_2	Γ_2	35	40	45
pH	τ_3	Γ_3	2	3	4

Table 2 Codified and natural Box–Behnken design of experiments and removal response efficiency influencing Lannate wastewater oxidation by dual oxidation system optimization

Run no.	Codified variables			Un-codified variables			Response (%, removal)	
	Γ_1	Γ_2	Γ_3	x_1	x_2	x_3	Experimental	Predicted
1	− 1	− 1	0	50	35	3	93.22	93.50
2	− 1	1	0	50	45	3	96.13	96.38
3	1	− 1	0	150	35	3	95.45	94.95
4	1	1	0	150	45	3	95.44	95.41
5	0	− 1	− 1	100	35	2	91.05	91.49
6	0	− 1	1	100	35	4	92.01	91.78
7	0	1	− 1	100	45	2	94.05	94.27
8	0	1	1	100	45	4	92.80	92.35
9	− 1	0	− 1	50	40	2	91.43	90.70
10	1	0	− 1	150	40	2	90.88	90.94
11	− 1	0	1	50	40	4	89.70	89.89
12	1	0	1	150	40	4	89.66	90.13
13	0	0	0	100	40	3	97.10	97.10
14	0	0	0	100	40	3	97.40	97.10
15	0	0	0	100	40	3	96.80	97.10

4 Experimental Investigation

4.1 Chemicals and Reagents

Commercial-grade Lannate, O-(methylcarbamoyl) oxime carbamate, was used as a model insecticide pollutant without further purification. Hydrogen peroxide (30% w/v), iron collected from coal industry wastewater effluent, is collected. Sodium hydroxide and sulfuric acid, all of analytical grade, were obtained from Sigma-Aldrich and were used as received from the supplier without further treatment for pH adjustment, if required.

Wastewater containing iron is produced from mining industry in Egypt, and iron is precipitated using a selective precipitation method. Silica-supported iron is prepared according to the previously cited techniques [14]. In such technique, iron material is selectively extracted and mixed with the silica particles. Thereafter, the mixture is dried at 103 °C in an electrical oven. The mixture is subjected for such process three replicates to assure the well mixing prior to the calcination at 500 °C in a furnace, and then, the amount of iron on silica particles is calculated.

4.2 Experimental Solar Reactor Setup and Analytical Determination

The pH of the photo-catalytically treated insecticide using modified silica-supported iron as a heterogeneous Fenton reaction source was adjusted to a set values of (3.0, 4.0, 6.5 or 7.0) by the use of diluted (1:9) H_2SO_4 or 0.1 N NaOH. Different amounts of the modified silica coated with iron-catalyst were added to 100 mL of pH-adjusted aqueous solution; thereafter, 30% concentration of H_2O_2 was added in a certain amounts while stirring with magnetic stirrer. Then, the samples were subjected to ultraviolet illumination (UV) for a specific reaction time under solar radiation via a parabolic trough solar collector mounted with tubular reactor as shown in Fig. 2. The aqueous solution augmented with reagents is circulated through the reactor, and samples are withdrawn at definite time intervals for analysis. The mixture is allowed to be separated before analysis using a microfilter (0.45 μm). The clarified filtered effluent samples are analyzed for Lannate residuals via Unico UV-2100 spectrophotometer (USA) at 231-nm maximum absorbance peak. A digital pH-meter, AD1030, Adwa Instruments (Hungary), is used for pH measurement. The optimal reactants parameters were applied to investigate the effects on the temperature by operating at various temperatures ranged from room temperature to 60 °C. All the experimental tests were repeated twice or thrice for duplicity purposes.

Solar experiments are extensively affected with the solar radiation intensity [23, 24]. From such point of view, solar intensity should be examined to investigate the maximal solar radiation periods to conduct the experimental work. Thus, the solar intensity is recorded at the location of conducting experiments where the solar collector with the tubular reactor is located at "*AMSEES* Laboratory, Menoufia University, Shebin El-Kom city at the north of Egypt." According to the previous reports [25, 26], Menoufia city is categorized as one

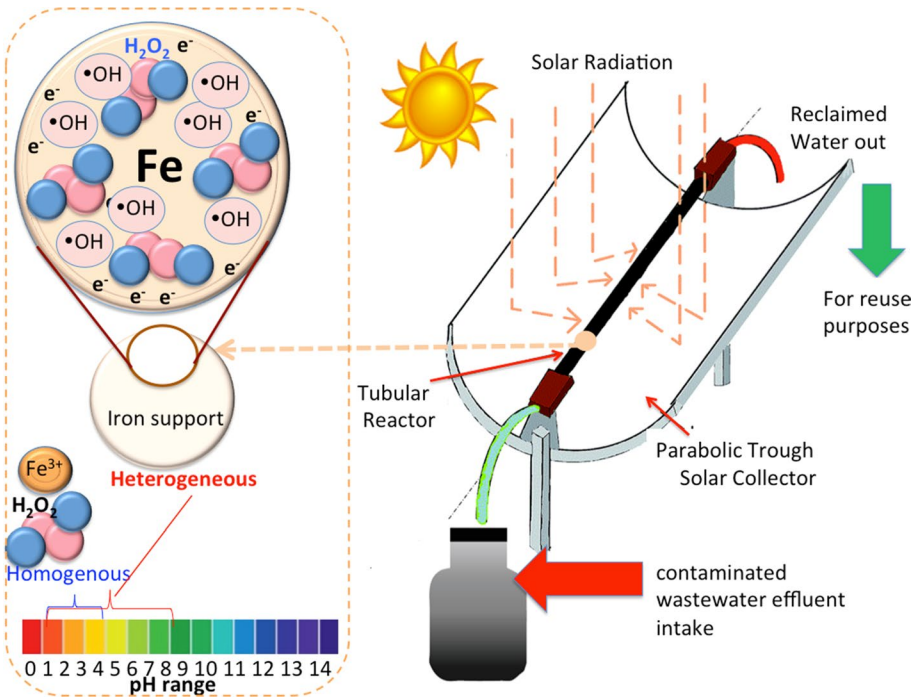

Fig. 2 Schematic diagram including the graphical representation of the experimental setup

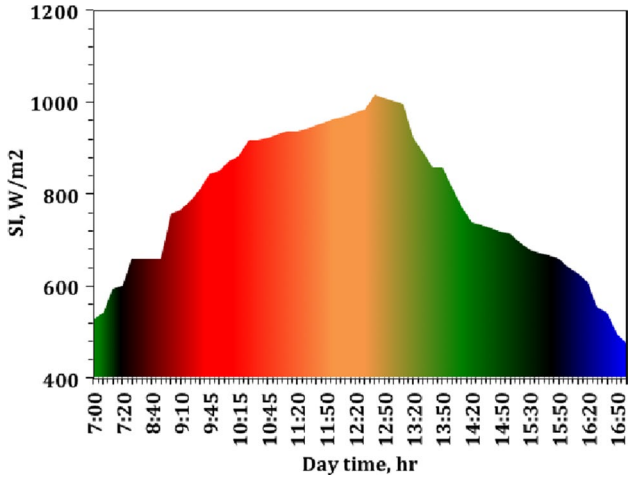

Fig. 3 Solar radiation intensity around the day at AMSEES Laboratory

of the most Egyptian abundant solar radiation cities. Such area is well endowed with sun energy and has high solar radiation, particularly at the summer period, which well suggests a place as a suitable option for conducting the experiments. The average sunshine periods over the place are over 10 h/day with the highest solar radiation recorded around the solar noon according to Fig. 3 being (1014 W/m^2). This value is declined before the sunset or not too high in the early morning at the time of conducting experiments as illustrated in Fig. 3.

4.3 Characterization Study

The crystal structure of the synthesized silica-coated iron catalyst was characterized by single-crystal X-ray diffraction, XRD measurements, which is conducted via a Bruker–Nonius Kappa CCD diffractometer with CuKα radiation source ($\lambda = 1.5406$). The measurement was performed under step-scan mode, and the registered intensities of the diffracted X-rays were detected every 0.026 Å over 2θ range of 4–80 Å. The diffractometer works at 40 kV with a scan step time of 0.6 s. Moreover, the Material Analysis was employed Using Diffraction (MAUD) program, version 2.54, for Riveted analysis. It is designed to retrieve simultaneously diffraction/reflectivity/fluorescence analysis program. The morphology of the synthesized samples was imaged by SEM micrograph using FE-SEM, Quanta FEG 250.

5 Results and Discussions

5.1 Structural and Morphological Characterization

The XRD diffractogram of the silica-supported iron catalysts is displayed in Fig. 4a. The crystalline phase of catalyst was identified, and the XRD patterns show several diffraction peaks. Rietveld refinement with the Maud software version was applied in order to analyze the diffraction pattern of the as-prepared silica-supported iron catalyst and is displayed in Fig. 4b. The crystal structures of hematite and quartz were considered to calculate the diffraction pattern. Figure 4 (b) displays the result of the refinement, which is a strong broadening result from the small crystalline domains of those phases. Thus, it could be concluded that the silica-supported iron catalyst consists of a crystalline silica core and hematite shell with only very small crystalline domains. This conclusion is supported by SEM measurements (Fig. 5) that display a highly crystalline core and an amorphous shell.

The morphology and microstructure of the samples were studied by SEM images. The SEM images of silica-coated iron sample are shown in Fig. 4 and the inset of Fig. 4. The images with different magnifications displayed that particles are in the nanometer range, nearly spherical shape. Rough surface structure may be formed due to the presence of iron on the surface of silica. Extensive flow through exposure of Lannate during the oxidation process may be smoothen the existing surface structure.

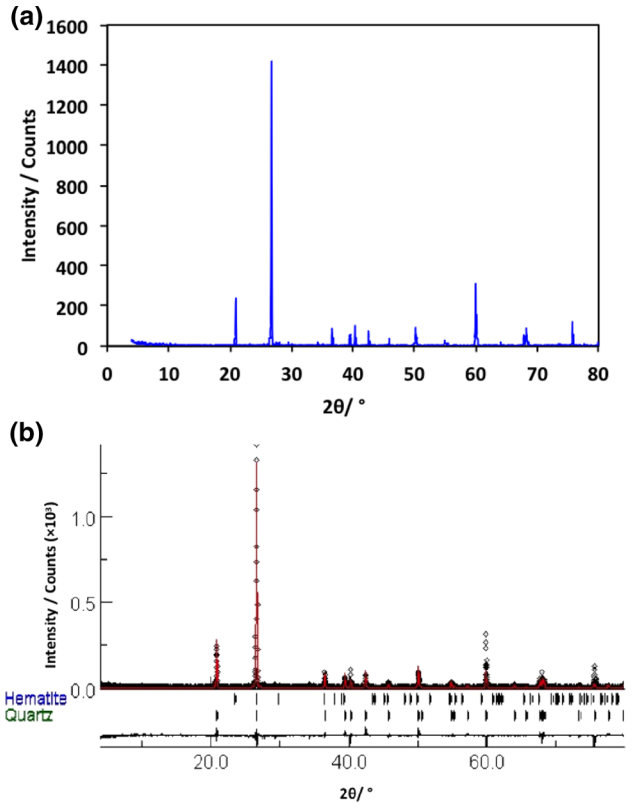

Fig. 4 **a** XRD patterns of silica-supported iron sample; **b** XRD pattern refinement using MAUD software for the silica-supported iron sample

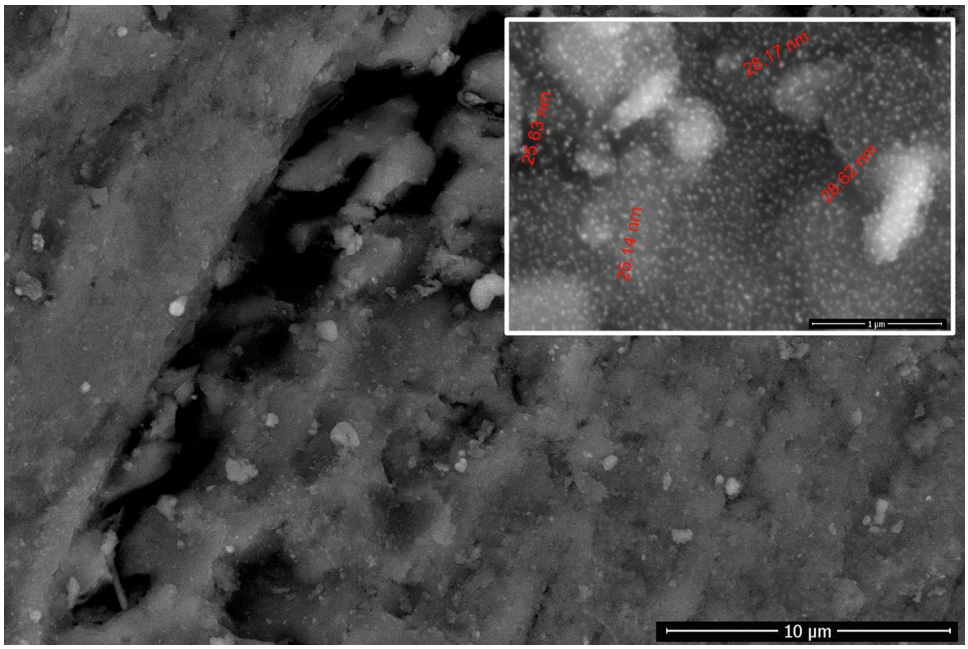

Fig. 5 SEM images of silica-supported iron sample at different magnification

5.2 Effect of Multivariate Parameters System

5.2.1 Effect of H_2O_2 Concentration

For generating hydroxyl radicals in the solar photo-Fenton's reaction, it is essential to decompose H_2O_2 in the presence of iron catalyst. In addition, it is crucial to maintain both H_2O_2 and iron catalyst concentrations minimum; meanwhile, their higher dosage decreases the reaction efficiency. Therefore, to examine the influence of H_2O_2 on the Fenton's oxidation of Lannate insecticide, experiments were conducted to investigate the influence of hydrogen peroxide dose on the reaction kinetics.

Figure 6a displays the effective Lannate oxidation process by varying the concentration of H_2O_2 over the range of 50–800 mg L^{-1}. The oxidation efficiency increases from 58 to 96% when the hydrogen peroxide concentration increases from 50 to 100 mg L^{-1}. Additionally, further H_2O_2 increase more than 100 mg L^{-1} results in a reduction in Lannate removal efficiency that declines to 82% when 200 mg L^{-1} of H_2O_2 was used. However, a further reduction in the oxidation efficiency with the increase in hydrogen peroxide dose was attained. This could be attributed by the excess hydrogen peroxide in the reaction medium, more than the optimal dose; H_2O_2 itself would act as ·OH scavenger rather than a generator, and result is producing HO_2 radicals as

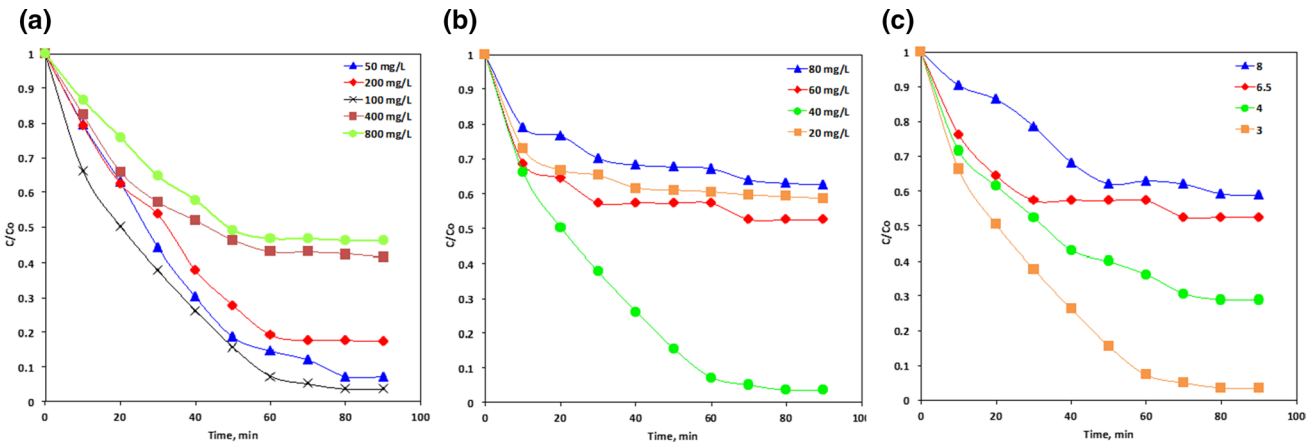

Fig. 6 Effect of operating parameters on AMD-Fenton oxidation system, **a** effect of H_2O_2 Lannate oxidation at pH 3.0 and iron 40 mg L^{-1}; **b** effect of iron concentration on Lannate oxidation at pH 3.0 and H_2O_2 100 mg L^{-1}; **c** effect of pH on Lannate oxidation at H_2O_2 100 mg L^{-1} and iron 40 mg L^{-1}

shown in Eq. (2). Such HO_2 radicals' species are less reactive compared to ˙OH radicals, and therefore, a negligible contribution is achieved. Also, the generated HO_2 radicals in the reaction medium react with the remaining ˙OH radicals according to Eq. (3). This investigation was previously recorded by the previous studies of Thabet et al. [27]. Thus, this results in a terminal effect in the Lannate removal rate.

$$H_2O_2 + HO^{\bullet} \rightarrow HO_2^{\bullet} + H_2O \quad (2)$$

$$HO_2^{\bullet} + HO^{\bullet} \rightarrow H_2O + O_2 \quad (3)$$

5.2.2 Effect of Iron Dose

In order to investigate the effect of iron dose on the Lannate removal rate, the iron concentration was increased in the reaction medium from 20 to 80 mg L^{-1}, while the other parameters are kept constant (H_2O_2 concentration was kept constant at 100 mg/L and the initial pH at 3.0). It is displayed in Fig. 6b increasing the iron concentration results in an increase in the rate of Lannate oxidation and the maximal rate reached to 96% when 40 mg L^{-1} is added. However, further iron addition more than 40 mg L^{-1} revealed a reduction in the removal of Lannate to 47 and 37% with the iron addition of 60 and 80 mg L^{-1}, respectively. Interestingly, adverse effects of excess iron doses on the solution were attained since the extra addition of the iron speciation in the aqueous medium hinders the OH radicals' performance Eqs. (4 and 5) [28]. This may be attributed by the ˙OH radicals trapped by excess iron ions. Hence, 40 mg/L is considered the optimum concentration needed for Lannate oxidation in the silica-supported iron Fenton system. Similar trend was previously investigated with Fenton process by Tony and Ali [29].

$$Fe^{2+} + OH^{\bullet} \rightarrow Fe^{3+} + OH^{-} \quad (4)$$

$$Fe^{2+} + OH_2^{\bullet} \rightarrow Fe^{3+} + OH_2^{-} \quad (5)$$

5.2.3 Effect of Initial pH

The aqueous stream pH is categorized as an important parameter that affects the Fenton's reaction system. The effect of initial aqueous matrix pH on the oxidation tendency of Lannate using silica-supported iron Fenton was assessed within pH range 3.0–8.0 [30]. The mean of the duplicated experimental results of Lannate concentration removals is plotted in Fig. 6c. The results are representing that pH considerably affected Lannate oxidation system, specifically under the acidic pH conditions. As it is seen from the curves in Fig. 6c, the Lannate concentration removal is increased from 41 to 96% as the pH altered from the alkali (8.0) solution to the acidic one. The reason that silica-supported iron-based Fenton system behaved differently at different solution pHs could be associated with the production of the ˙OH radicals. This confirms that both the iron speciation and hydrogen peroxide decomposition are affected by the pH value. In addition, according to the previously cited literature [31–36], the rate of hydroxyl radicals' production is strongly enhanced at the acidic pH medium. Optimal pH plays an important role on the •OH production; meanwhile, above or below this limit reduces the reactive radicals formation. Fe^{3+} could be produced at the high pH values as well as other complexes such as (FeOOH) that have low catalytic activity compared to Fe^{2+}. Moreover, below the optimal pH, more H^+ is generated in the reaction medium, which is further scavenging the •OH radicals' activity according to Eq. (6) [14, 37]. Hence, it is essential to control the pH of the aqueous Lannate solution in this narrow acidic range [33, 38].

$$H^+ + OH^{\bullet} + e^- \rightarrow H_2O \quad (6)$$

5.3 Effect of Lannate Concentration

In the indusial and agricultural wastewater discharge basis, the pollutant loading in aqueous streams of wastewater treatment facilities changes in a daily basis. Thus, from this concept, it is imperative to evaluate the Fenton's oxidation dependence on the Lannate load. Therefore, Lannate loading is varied from 50, 60, 80 and 100 ppm to investigate the oxidation efficiency with increasing the Lannate concentration, while all other experimental conditions kept at its optimum values (pH 3.0; H_2O_2 100 and iron 40 mg L^{-1}, respectively). The results displayed in Fig. 7 that are the average of three replicates indicate that increasing the Lannate concentration results in a reduction in the Lannate oxidation efficiency reached to 2% when the Lannate loading was 100 ppm; however, the removal increased to 96% when the Lannate loading is 50 ppm. This may be related to the short life time of •OH radicals' species that is considered the main controlling stage of the Fenton's oxidation reaction generally raising the tendency of collision between the radical species and contaminates molecules in wastewater matrix. Thus, the result is improving the rate of Lannate oxidation. On the contrary, the increase in the Lannate concentration is leading to a reduction in the Fenton's oxidation efficiency. This is because the number of active sites of the silica-supported Fenton's system reaction is inadequate for the too high Lannate loading. Moreover, the high loaded Lannate in the aqueous stream results in a decrease in the light absorption via H_2O_2 that are needed for the photo-Fenton system thereby rendering the OH radical species. It is noteworthy to mention that more

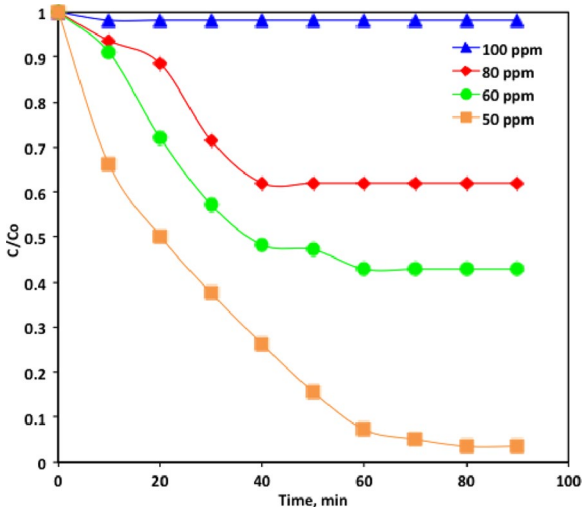

Fig. 7 Effect of Lannate loading on the oxidation rate (operating conditions at pH 3.0; H_2O_2 100 mg L^{-1} and iron 40 mg L^{-1})

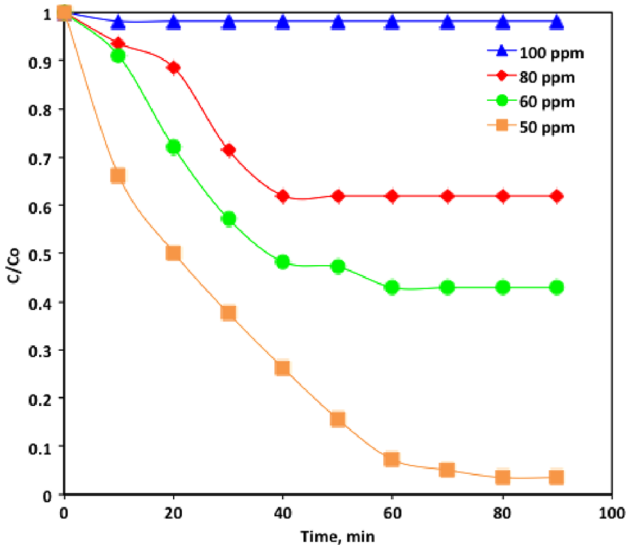

Fig. 8 Effect of temperature on sillica-supported iron Fenton oxidation system

time is required to reach the needed treatment efficiency. Also, treating higher Lannate loading at the same catalysts and reagents concentrations it could not reach to a higher removal rate. Such observation of decreasing the removal rate with increasing the initial contaminate loading in aqueous stream is previously recorded by Najjar et al. [39] and Tony et al. [40].

5.4 Temperature Effects on Kinetics and Thermodynamic Parameters

In the catalytic oxidation reactions, temperature effect is signified as a significant factor that affects reaction rates. In order to investigate the influence of temperature on reaction kinetics, Lannate oxidation experiments over a temperature ranged from 32 to 60 °C were undertaken. The data displayed in Fig. 8 illustrates the reduction in Lannate oxidation efficiency is decreased from 96 to only 41% over the temperature range investigated. Such trend could be related to the H_2O_2 reagent that could be thermally decomposed to O_2 and H_2O rather than producing hydroxyl radicals. Moreover, the much too high temperature elevation accelerates the presence of iron leachate in the medium and the iron catalyst could be lost [41]. Moreover, the high temperature could deteriorate the heterogeneous catalyst support material, i.e., silica, thus losing the iron catalyst activity, which could be decomposed into fine particles.

Hence, the overall Lannate oxidation rate is temperature-dependent technology. Several investigators [41–44] have been previously described the experimental evidence for the dependency of catalytic oxidation on temperature. Also, the earlier results recorded also verified that the high temperature values decline Fenton and Fenton like oxidation efficiency. Furthermore, Soares et al. [45] and Gogate and Pandit [46] reported that the catalytic oxidation of the Fenton's reaction has an optimal temperature value that is a controlling step for such reaction.

Generally, Fenton oxidation reaction is categorized as a complex reaction in nature since it includes a simultaneous oxidation and coagulation processes. Moreover, the reaction includes many reacting species. Hence, the result is a complicated reaction and investigating its kinetics is also not simple. The zero, first and second reaction kinetic models are used to examine the reaction kinetics at different temperatures (32, 40, 50 and 60 °C). The corresponding for the zero, first and second reaction kinetic models of kinetic constants (k_0, k_1 and k_2, respectively) is investigated and the data are listed in Table 3. The regression coefficients (r^2) values are explored and applied to examine the suitable kinetic order. According to the results listed in Table 3 from this investigation it signifies that the process generally follows first-order kinetics. Furthermore, the lowest value of half-life time ($t_{1/2}$) is corresponding to the 32 °C reaction temperature (Table 4). Such investigation is previously stated in similar studies using homogeneous Fenton systems [46, 47].

In order to further understand the temperature effect on the Lannate oxidation system using silica-supported iron-based heterogeneous Fenton reaction, the thermodynamic activation parameters were attained and are listed in Table 5. The thermodynamic parameters were established by Arrhenius equation that is based on the first-order kinetic model according to Eq. (7):

Table 3 Fitted rate constants for municipal wastewater oxidation reaction*

Kinetic model	Parameter	Temperature			
		32 °C	40 °C	50 °C	60 °C
Zero-order ($C_t = C_o - k_o t$)	k_0 (min^{-1})	0.4987	0.3776	0.2041	0.1915
	$t_{1/2}$ (min)	50.46	66.64	123.29	131.40
	r^2	0.85	0.87	0.64	0.69
First-order ($C_t = C_o - e^{k_1 t}$)	k_1 (min^{-1})	0.0431	0.0172	0.014	0.0087
	$t_{1/2}$ (min)	79.65	49.5	40.29	16.09
	r^2	0.98	0.98	0.9	0.91
Second-order $\left(\left(\frac{1}{C_t}\right) = \left(\frac{1}{C_0}\right) - k_2 t\right)$	k_2 (L mg^{-1} min^{-1})	0.0067	0.0007	0.0002	0.0001
	$t_{1/2}$ (min)	2.96	28.38	99.34	198.69
	r^2	0.86	0.99	0.76	0.78

*k_0, k_1, k_2: kinetic rate constants of zero-, first- and second-order reaction kinetic models; C_o and C_t: Lannate concentrations at initial and time t; t: time; r^2: correlation coefficient; $t_{1/2}$ half-life time

Table 4 Thermodynamic parameters for Lannate wastewater oxidation over silica-supported iron Fenton system*

Temperature	E_A = 34.54 kJ/mol		
	$\Delta H°$	$\Delta S°$	$\Delta G°$
32 °C	32.00	− 166.31	82.73
40 °C	31.94	− 177.05	87.36
50 °C	31.86	− 182.44	90.78
60 °C	31.77	− 189.86	94.99

*Activation energy (E_A), the variation in activation enthalpy $\Delta H°$ (kJ/mol), the variation in activation entropy $\Delta S°$ (J/mol), and the variation in the free energy of activation $\Delta G°$ (kJ/mol)

$$\left(\ln k_F = \ln A - \frac{E_a}{\mathrm{RT}}\right) \tag{7}$$

where A is the pre-exponential factor constant; E_a is the energy of activation (kJ mol^{-1}); R is the universal gas constant (8.314 J mol^{-1} K^{-1}); and T is the absolute temperature (K). The slope of the linear plot of $ln\ k_F$ versus 1/T in Fig. 9 is ($-E_a/R$); such slope could be applied to investigate the value of E_a. Eyring equation (Eq. (8)) [51] is used to investigate the thermodynamic parameters

$$k_F = \frac{k_B T}{h} e^{\left(-\frac{\Delta G^\circ}{\mathrm{RT}}\right)} \tag{8}$$

where k_B and h are Boltzmann and Planck's constants, respectively. In addition, the enthalpy ($\Delta H°$) and the entropy ($\Delta S°$) of activation could be investigated from the relation attained in Eqs. (9) and (10), respectively [52]:

$$\Delta H^\circ = E_a - RT \tag{9}$$

$$\Delta S^\circ = (\Delta H^\circ - \Delta G^\circ)/T \tag{10}$$

Table 4 displays the thermodynamic results attained from such relations. Analysis of the results indicates the non-spontaneous oxidation process since $\Delta G° > 0$, with increasing its degree of non-spontaneity with the temperature increase. Also, positive $\Delta H°$ values assessed the endothermic nature of the Fenton oxidation reaction. Additionally, the non-spontaneous oxidation nature of the reaction is verified from the negative values of entropy of activation ($\Delta S°$), which displayed a decrease in the degree of freedom of the Lannate molecules and maintained a high ·OH yield. This investigation correlates the endothermic Fenton oxidation process, and non-spontaneous nature is in accordance with that previously stated by Argun and Karatas [53], Tony and Lin [47] and Pourali et al. [54]. Furthermore, the data investigated that the Lannate oxidation via such silica-supported iron as a modified heterogeneous Fenton system typically proceeds at 34.54 kJ mol^{-1}, which is recognized as a low energy barrier. Also, previous results of Ahmadi et al. [55] reported the low energy barrier of 45.84 $kJmol^{-1}$ is the activation energy of the Fenton's system for oxidizing dye.

5.5 BBD Factorial Design and ANOVA testing

The effect of the most three independent critical parameters in the Fenton oxidation system, namely H_2O_2 concentration, iron catalyst dose and pH, on Lannate removal was simulated using Box–Behnken design (BBD) model tabulated in Table 2. The data collected from this factorial design were processed and fitted to quadratic polynomial model equation. The quadratic polynomial model equation form validates the associated response function Lannate removal (%γ) as follows [56]:

$$\begin{aligned}\gamma = {} & 97.1 + 0.12\Gamma_1 + 0.84\Gamma_2 - 0.41\Gamma_3 \\ & - 2.05\Gamma_1^2 - 0.73\Gamma_1\Gamma_2 + 0.13\Gamma_1\Gamma_3 \\ & + 0.01\Gamma_2^2 - 0.55\Gamma_2\Gamma_3 - 4.63\Gamma_3^2\end{aligned} \tag{11}$$

Using the SAS software and the models' multivariate statistical analysis (ANOVA) allows determining the correlation between the studied variables and the maximized Lannate removal response. Table 6 illustrates the ANOVA results; the data in Table 6 revealed that the quadratic polynomial model is highly significant with a satisfied correlation coefficient values, r^2. Commonly, from the statistics determination the model is acceptable if the coefficient of determination, r^2, is more than 80% [47]. Also, the model is well fitted when a large value of *Fisher test* is attained which is much greater than unity besides a minimal p-value

Table 5 Comparison of various treatment methodologies for pesticide-containing wastewater effluents abatement*

Treatment system	Catalyst	Pesticide name	Experimental conditions	Removal, %	Refs.
Homogeneous Fenton system	Silica-supported iron	Lannate pesticide	23 °C, pH 3, H_2O_2 0.015 M, Fe^{2+} 5.0×10^{-4} M, 90 min	98%	Current study
Homogeneous Fenton system	$FeSO_4$ heptahydrate	Paraquat pesticide	20–30 °C, pH 2.8, H_2O_2 0.103 mg/L, Fe 45 mg/L, 8 h	100%	[48]
Heterogeneous Fenton-like-microwave system	$Cu/Cu_2O/CuO/MW$	Methomyl pesticide	$H_2O_2$5000 mg/L, catalyst 3.0 g/L, pH 6.5, MW power 400 W	91%	[37]
Heterogeneous Fenton-like-UV system	n-CuO	Carbamate methomyl pesticide	*n-CuO* 75 mg/L, H_2O_2 395 mg/ L, pH 6.5, UV lamp (15 W, 253.7 nm)	85%,	[36]
Heterogeneous TiO_2 (amorphous & anatase)	UV/TiO_2	Methomyl pesticide	pH 3.0, TiO_2 20 mg/ L	100%	[38]
Heterogeneous photo-Fenton-like	UV/Magnetite nanoparticles	Carbamate pesticide	C_o 50 mgL^{-1}, pH 3, Fe^{2+} 40 mgL^{-1}, H_2O_2 50 mgL^{-1}, 60 min	90%	[49]
Heterogeneous photo-Fenton-like	Solar/Magnetite nanoparticles	Carbamate pesticide	C_o 50 mgL^{-1}, pH 3, Fe^{2+} 44 mgL^{-1}, H_2O_2 52 mgL^{-1}, 170 min	96.5%	[49]
Heterogeneous photo-Fenton	US-Fe^{2+}	Methomyl pesticide	C_o 25 ppm, pH 2.5, Fe^{2+} / H_2O_2 1:30 mM 18 min		[50]
Photo-Fenton	UV/Fe	Lannate pesticide	Co 16.22 ppm, pH 3.7, Fe 5 g/L; 4 h	100%	[34]
Catalytic photooxidation	ZnO/UV	Lannate pesticide	Co 16 ppm, pH 5.6, ZnO 2000 mg/L, 240 min	80%	[35]
Photo-Fenton	UV/Fe	Methomyl pesticide	50 ppm, pH 3.0, Fe 40 mg/L catalyst; 80 min	72%	[4]

*UV: ultraviolet; US: ultrasonic; MW: microwave power

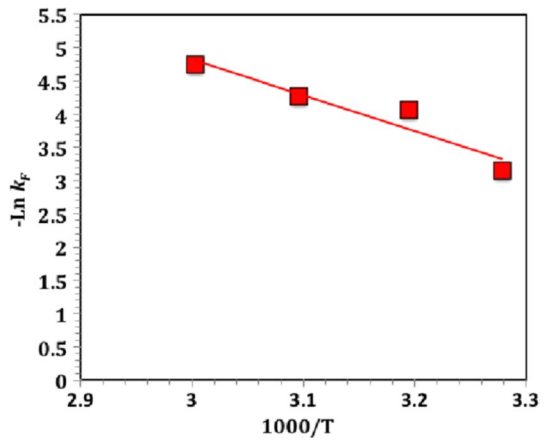

Fig. 9 Plot of ln k_F versus 1000/T for Lannate oxidation reaction (solid line represents least-squares fitting)

Table 6 ANOVA for the regression model and the respective models terms*

Source	DF	SS	MS	F	Pr > F
Model	9	101.2152	11.24613	32.49248	0.0006
Error	5	1.73	0.35		
Total	14	102.9458			
r^2	98.32%				
Adj-r^2	95.29%				

*DF: Degree of freedom; SS: Sum of Squares; MS: Mean Squares; F-value; Fisher test; Pr: Probability; r^2: Coefficient of correlation; Adj-r^2 adjusted r^2

(< 0.05) is achieved [57]. The value coefficient of determination of the proposed model values is 98.32%, which indicates the fitness of attained model. Since low Pr > F value is attained 0.0006, the ANOVA results reveal a high correlation between the response and the variables. Thus, from the ANOVA test the proposed simulated model is well fitted the experimental data.

The interactions between the studied parameters, i.e., hydrogen peroxide, catalyst doses and pH, are essential to be recognized. To do so, the 3D surface and 2D contour graphs

are used to describe the investigated regression model and the graphs are displayed in Fig. 10a–c. Such graphs illustrate the influence of each two independent parameters studied on the Lannate removal.

According to Fig. 10a, the Lannate oxidation efficiency that is verified through its concentration elimination is steadily improved with the increased reagent dosage of both reagents H_2O_2 and silica-supported iron catalyst. The main attribution of this trend is the hydroxyl radicals' yield in the wastewater that is increased with the silica-supported dosage and hydrogen peroxide increase. But, after a certain reagent limit, the Lannate oxidation rate is deduced. This significant relation could be related to the over catalyst dosing which acts as a radical scavenger rather than a producer. Moreover, the extent of 3D surface curvature plot is a signal for the degree of exaggerated on the response (γ, %) as the more circular contour curvature categorizes a weaker interaction effect. Moreover, as shown in Fig. 10b, c, the system is highly sensitive to the pH change compared to the other parameters studied. Further, the model equation (Eq. (10)) is applied to investigate the relation between the predicted and experimental responses that indicated the values obtained were close to linearity that means the data were accurate and reliable according to the results displayed in Fig. 11.

Also, the numerical simulated optimization of the system is further attained through Mathematica software (version V 5.2) and the optimum values recorded are 103, 45 mg L^{-1} for H_2O_2 and catalyst, respectively, at pH 2.8. Further, for the object of confirmation, the recorded predicted optimal values were used to precede real experiments through duplicates of experiments and original response values are compared with the simulated ones, which reached the Lannate removal to 98%. The experimental data showed high correlation between the model predictions and the experimental

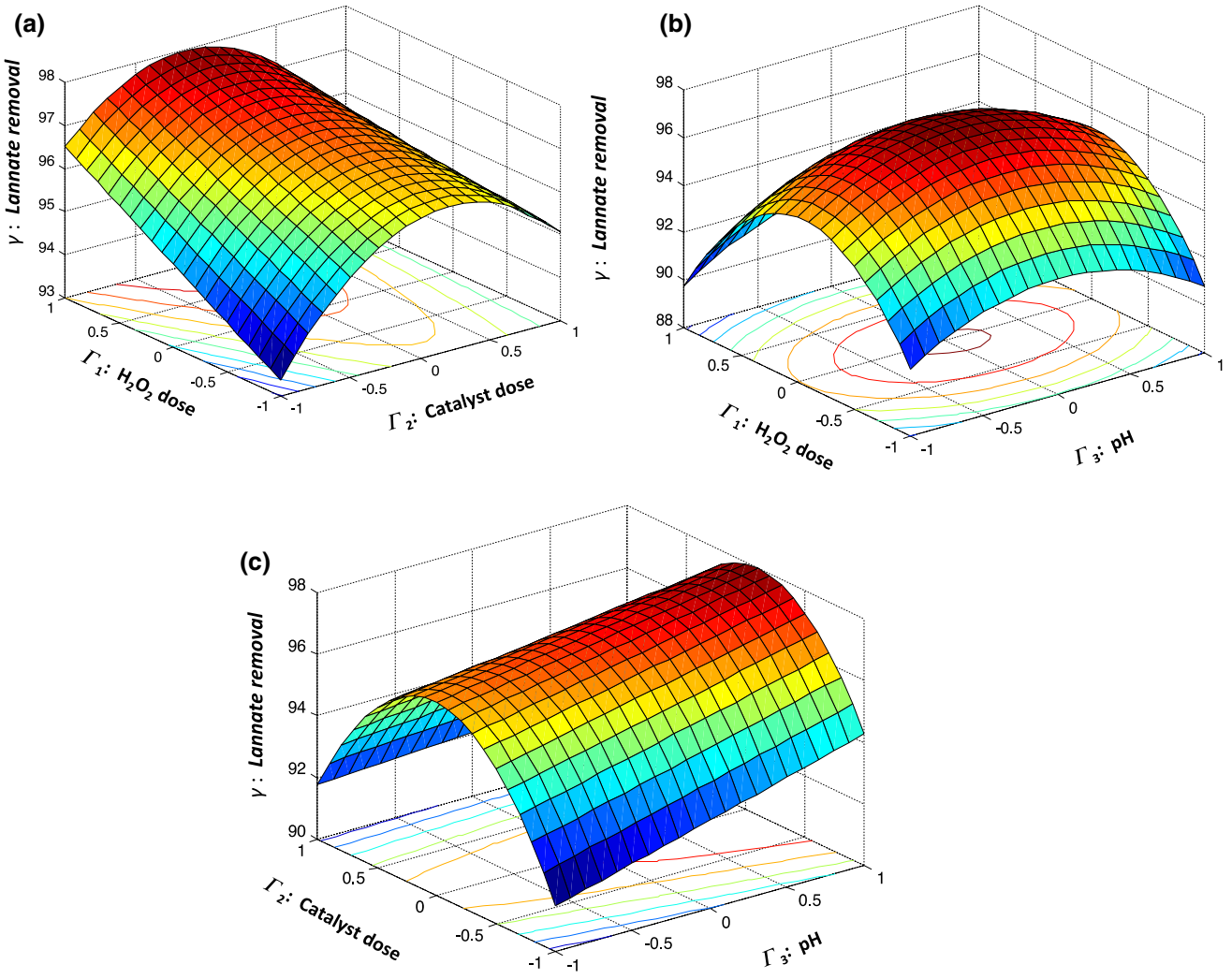

Fig. 10 3D Surface augmented with contour plots of the factorial design for Lannate oxidation, **a** hydrogen peroxide versus catalyst dose; **b** hydrogen peroxide versus pH and **c** catalyst dose versus pH

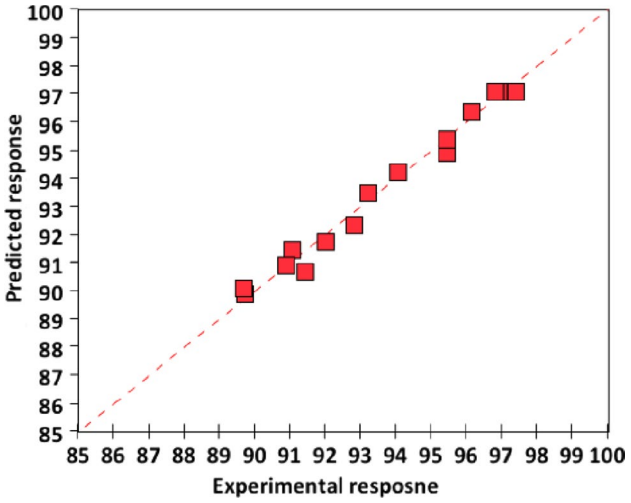

Fig. 11 Graphical representation of experimental and predicated responses

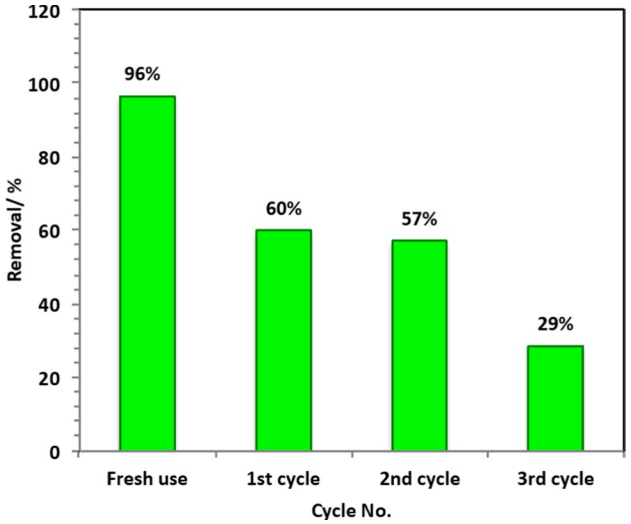

Fig. 12 Reusability assays of the silica iron-based catalyst

results that further verifies the goodness of fitness of the model for the results besides the ANOVA data.

5.6 Comparison of Treatment Methodologies

Comparison the oxidation efficiencies between the experimental data attained from the current study in using silica-supported iron as a heterogeneous photocatalyst as a source of Fenton reaction and those reported in the literature in treating pesticide in aqueous effluent with the classic Fenton and other oxidants is listed in Table 5. Encouragingly, heterogeneous photo-Fenton shows almost complete 98% removal rate compared to removal ranged from 72 to 100% with other systems. However, lower reaction time was needed for the silica-supported iron-based Fenton system in the current study comparable to other systems. An efficient superior treatment is recorded for the current study since the solar economic activation source is used. It should be mentioned that the other systems contain a fresh iron or catalyst source compared to the application of the waste iron in the current investigation to introduce the opportunity of a cradle-to-cradle technology for treating via a cost-efficient way. Moreover, such other studies exhibited some disadvantages such as the long reaction time and quantities of chemical agents in comparison with the current Fenton system. Moreover, it is noteworthy to mention that the current system is a heterogeneous recyclable sustainable catalyst that could be applied of successive times use. Also, the sustainability of the catalyst makes it possesses the opportunity of easily removable from the final effluents to avoid the final sludge formation. Thus, this is recommending such technology for Lannate insecticide elimination.

5.7 Recyclability

Silica-supported iron catalyst stability and recyclability are of greater interest for its long-term applicability in the science of aqueous waste treatment reclamation. From this regard, the heterogeneous iron-based material is checked for its stability since it possesses a superior separation nature as a heterogeneous catalyst. The catalyst is separated and then it is subjected for a successive washing with distilled water prior to oven drying at 105 °C. Thereafter, the separated, recovered and then regenerated material is applied for reuse. The data of the experimental results after successive process use are displayed in Fig. 12. The results demonstrated that a well catalytic activity is attained during the range of experimental study till the third cycle of use. Such results verify the high stability of the material after repetitive second use for 57% which declined to 28% after the third cycle. Thus, the study verified their promising sustainability for the use in treating industrial wastewater effluents. The typical oxidation percentage of the Lannate oxidation based on the successive cycles of using silica-supported iron-based Fenton material is presented in Fig. 12.

6 Conclusion

The current investigation attempted to explore the applicability of modified Fenton system for oxidizing Lannate insecticide from aqueous effluent. The experimental results of the study revealed that silica-supported iron provides higher solar Fenton reaction efficiencies with minimum energy and chemicals consumption. The Lannate concentration as target efficiency was found to be a function of the initial pH, H_2O_2 and catalyst doses. Box–Behnken factorial design has been successfully employed

for process optimization, and the optimum operating values were 45 and 103 mg L^{-1} of catalyst and H_2O_2, respectively, at 90 min of reaction time and acidic pH (2.8) conditions. The pseudo-first-order kinetic model is well fitted the experimental results. Generally, the results obtained verify the significant role of the recyclable silica-supported heterogeneous material in oxidizing Lannate molecules from aqueous effluents. Such experimental data, derived from the synesthetic wastewater, add to a knowledge base for treating real textile wastewater matrix treatment applications. However, the developments of solar photo-Fenton for industrial-scale applications still require further research as well as novel advances to enhance the efficiency in economic overview. Interestingly, it is notable that large land area is needed for solar reactors that are added to the economic cost of the treatment facility. Such consideration makes the process expensive. Conversely, low maintenance cost of the solar installation is considered the merit that declines the total treatment cost.

Funding Open access funding provided by The Science, Technology & Innovation Funding Authority (STDF) in cooperation with The Egyptian Knowledge Bank (EKB). The author(s) received no specific funding for this work.

Data Availability All data generated or analyzed during this study are included in this published article.

Declarations

Conflict of interest The authors confirm that there is no conflict of interest to declare.

References

1. Van Scoy, A.R., Yue, M., Deng, X., Tjeerdema, R.S.: Environmental fate and toxicology of methomyl. Rev. Environ. Contam. Toxicol. 93–109 (2013).
2. Ilyas, S., Bukhari, D.A., Rehman, A.: Shot communications-decolorization of synozol red 6hbn by yeast, candida tropicalis 4s, isolated from industrial wastewater. Pak. J. Zool. **47**(4) (2015).
3. Ashour, E.A.; Tony, M.A.: Equilibrium and kinetic studies on biosorption of iron (ii) and iron (iii) ions onto eggshell powder from aqueous solution. Appl Eng. **1**(3), 65–73 (2017)
4. Rahma Hussien Thabet, M.K.F.; El Sherbiny, S.A.; Tony, M.A.: Solar concentration for pesticide-containing wastewater combat: can solar energy meet a green costless? In: IEECE 3rd International Conference of Chemical, Energy and Environmental Engineering (2021)
5. Feng, H.E.; Le-Cheng, L.E.I.: Degradation kinetics and mechanisms of phenol in photo-Fenton process. J. Zhejiang Univ. Sci. A **5**(2), 198–205 (2004)
6. Farré, M.; Fernandez, J.; Paez, M.; Granada, L.; Barba, L.; Gutierrez, H.; Pulgarin, C.; Barceló, D.: Analysis and toxicity of methomyl and ametryn after biodegradation. Anal. Bioanal. Chem. **373**(8), 704–709 (2002)
7. Khan, M.A.N.; Siddique, M.; Wahid, F.; Khan, R.: Removal of reactive blue 19 dye by sono, photo and sonophotocatalytic oxidation using visible light. Ultrasonics Sonochem. **26**, 370–377 (2015)
8. Khedher, M., Mossad, M., El-Etriby, H.K.: Treatment of colored wastewater from textile industry using electrocoagulation process مادختسابجيسنلا ةعانصنم ةجتانلا ةنوللملا فرصلا ةايم ةجلاعم يبرهكلا بيورتلا
9. Maroudas, A.; Pandis, P.K.; Chatzopoulou, A.; Davellas, L.-R.; Sourkouni, G.; Argirusis, C.: Synergetic decolorization of azo dyes using ultrasounds, photocatalysis and photo-Fenton reaction. Ultrasonics Sonochem. **71**, 105367 (2021)
10. Ashour, A.; Tony, M.A.; Purcell, P.J.: Use of agriculture-based waste for basic dye sorption from aqueous solution: kinetics and isotherm studies. Am. J. Chem. Eng. **2**(6), 92–98 (2014)
11. Mandour, R.: Distribution and accumulation of heavy metals in lake Manzala, Egypt. Egypt. J. Basic Appl. Sci. **8**(1), 284–292 (2021)
12. Tony, M.A.; Purcell, P.J.; Zhao, Y.; Tayeb, A.M.; El-Sherbiny, M.F.: Kinetic modeling of diesel oil wastewater degradation using photo-fenton process. EEMJ **14**(1) (2015).
13. Li, Y.; Jin, Z.; Li, T.; Li, S.: Removal of hexavalent chromium in soil and groundwater by supported nano zero-valent iron on silica fume. Water Sci. Technol. **63**(12), 2781–2787 (2011)
14. Tony, M.A.; Lin, L.-S.: Iron coated-sand from acid mine drainage waste for being a catalytic oxidant towards municipal wastewater remediation. Int. J. Environ. Res. (2021). https://doi.org/10.1007/s41742-020-00309-7
15. Tony, M.A.: Paradigms of homo/heterogonous Fenton systems incorporating' solar energy 'based on' emerging pollutants' removal–challenges, advancements and visualized bibliometric analysis. Int. J. Environ. Anal. Chem. 1–32 (2021).
16. Zou, Y.; Wang, X.; Khan, A.; Wang, P.; Liu, Y.; Alsaedi, A.; Hayat, T.; Wang, X.: Environmental remediation and application of nanoscale zero-valent iron and its composites for the removal of heavy metal ions: a review. Environ. Sci. Technol. **50**(14), 7290–7304 (2016)
17. Ali, F.; Khan, S.B.; Kamal, T.; Alamry, K.A.; Asiri, A.M.; Sobahi, T.R.A.: Chitosan coated cotton cloth supported zero-valent nanoparticles: simple but economically viable, efficient and easily retrievable catalysts. Sci. Rep. **7**(1), 1–16 (2017)
18. Joshi, S.; Garg, V.K.; Kataria, N.; Kadirvelu, K.: Applications of Fe3o4@ ac nanoparticles for dye removal from simulated wastewater. Chemosphere **236**, 124280 (2019)
19. Liu, L.; Liu, S.; Mishra, S.B.; Sheng, L.: An easily applicable and recyclable Fenton-like catalyst produced without wastewater emission and its performance evaluation. J. Clean. Prod. **234**, 653–659 (2019)
20. Hamd, W.S.; Dutta, J.: Heterogeneous photo-fenton reaction and its enhancement upon addition of chelating agents. Nanomater. Detect. Removal Wastewater Pollut. 303–330 (2020).
21. Abdollahzadeh, H.; Fazlzadeh, M.; Afshin, S.; Arfaeinia, H.; Feizizadeh, A.; Poureshgh, Y.; Rashtbari, Y.: Efficiency of activated carbon prepared from scrap tires magnetized by Fe3o4 nanoparticles: characterisation and its application for removal of reactive blue19 from aquatic solutions. Int. J. Environ. Anal. Chem. 1–15 (2020).

22. Ye, Z.; et al.: Mechanism and stability of an Fe-based 2D MOF during the photoelectro-Fenton treatment of organic micropollutants under UVA and visible light irradiation. Water Res. **184**, 115986 (2020)
23. Marcelino, R.B.P.; Queiroz, M.T.A.; Amorim, C.C.; Leão, M.M.D.; Brites-Nóbrega, F.F.: Solar energy for wastewater treatment: review of international technologies and their applicability in Brazil. Environ. Sci. Pollut. Res. **22**(2), 762–773 (2015)
24. Cetinkaya, S.G.; Morcali, M.H.; Akarsu, S.; Ziba, C.A.; Dolaz, M.: Comparison of classic Fenton with ultrasound Fenton processes on industrial textile wastewater. Sustain. Environ. Res. **28**(4), 165–170 (2018)
25. Hussein, T.A.T.; Ahmed, T.: Estimation of hourly global solar radiation in Egypt using mathematical model. Int. J. Latest Trends Agric. Food Sci. **2**(2), 74–82 (2012)
26. Tony, M.A.; Mansour, S.A.: Solar photo-fenton reagent with nanostructured iron oxide for Bismarck dye oxidation: an Egyptian apparel case study. Int. J. Environ. Sci. Technol. **17**(3), 1337–1350 (2020)
27. Thabet, R.H.; Fouad, M.K.; Ali, I.A.; El Sherbiney, S.A.; Tony, M.A.: Magnetite-based nanoparticles as an efficient hybrid heterogeneous adsorption/oxidation process for reactive textile dye removal from wastewater matrix. Int. J. Environ. Anal. Chem. 1–23 (2021).
28. Tony, M.A.: Low-cost adsorbents for environmental pollution control: a concise systematic review from the prospective of principles, mechanism and their applications. J. Dispers. Sci. Technol. 1–23 (2021).
29. Tony, M.A.; Ali, I.A.: Mechanistic implications of redox cycles solar reactions of recyclable layered double hydroxides nanoparticles for Remazol brilliant abatement. Int. J. Environ. Sci. Technol. 1–18 (2021).
30. Thabet, R.H.; Tony, M.A.; El Sherbiny, S.A.; Ali, I.A.; Fouad, M.K.: Catalytic oxidation over nanostructured heterogeneous process as an effective tool for environmental remediation. IOP Conf. Ser. Mater. Sci. Eng. **975**, 012004 (2020)
31. Devi, L.G.; Raju, K.S.A.; Kumar, S.G.; Rajashekhar, K.E.: Photodegradation of di azo dye bismarck brown by advanced photo-Fenton process: influence of inorganic anions and evaluation of recycling efficiency of iron powder. J. Taiwan Inst. Chem. Eng. **42**(2), 341–349 (2011)
32. Ashour, E.A.; Tony, M.A.: Eco-friendly removal of hexavalent chromium from aqueous solution using natural clay mineral: activation and modification effects. SN Appl. Sci. **2**(12), 1–13 (2020)
33. Zhao, Y.Q.; Keogh, C.; Tony, M.A.: On the necessity of sludge conditioning with non-organic polymer: AOP approach. J. Residuals Sci. Technol. **6**(3), 151–155 (2009)
34. Tomašević, A.; Kiss, E.; Petrović, S.; Mijin, D.: Study on the photocatalytic degradation of insecticide methomyl in water. Desalination **262**(1–3), 228–234 (2010)
35. Tomašević, A.; Mijin, D.; Gašic, S.; Kiss, E.: The influence of polychromatic light on methomyl degradation in tio2 and ZnO aqueous suspension. Desalin. Water Treat. **52**(22–24), 4342–4349 (2014)
36. Tony, M.A.; Purcell, P.J.; Mansour, S.A.: Photodegradation and box-Behnken design optimization for methomyl using Fenton process based on synthesized CuO nanocrystals via facile wet chemical technique. Chem. Eng. Commun. 1–15 (2020).
37. Tony, M.A.; Mansour, S.A.: Microwave-assisted catalytic oxidation of methomyl pesticide by cu/cu 2 o/cuo hybrid nanoparticles as a fenton-like source. Int. J. Environ. Sci. Technol. **17**(1), 161–174 (2020)
38. Tony, M.A.; Mansour, S.A.: Synthesis of nanosized amorphous and nanocrystalline tio2 for photochemical oxidation of methomyl insecticide in aqueous media. Water Environ. J. **34**, 239–249 (2020)
39. Najjar, W.; Chirchi, L.; Santos, E.; Ghorhel, A.: Kinetic study of 2-nitrophenol photodegradation on al-pillared montmorillonite doped with copper. J. Environ. Monit. **3**(6), 697–701 (2001)
40. Tony, M.A.; Lin, L.S.: Performance of acid mine drainage sludge as an innovative catalytic oxidation source for treating vehicle-washing wastewater. J. Dispersion Sci. Technol. (2020). https://doi.org/10.1080/01932691.2020.1813592
41. Titouhi, H.; Belgaied, J.-E.: Heterogeneous fenton oxidation of ofloxacin drug by iron alginate support. Environ. Technol. **37**(16), 2003–2015 (2016)
42. Liou, R.-M.; Chen, S.-H.; Hung, M.-Y.; Hsu, C.-S.; Lai, J.-Y.: Fe (iii) supported on resin as effective catalyst for the heterogeneous oxidation of phenol in aqueous solution. Chemosphere **59**(1), 117–125 (2005)
43. Tony, M.A.; Lin, L.-S.: Attenuation of organics contamination in polymers processing effluent using iron-based sludge: process optimization and oxidation mechanism. Environ. Technol. 1–10 (2020).
44. Thabet, R.H.; Fouad, M.K.; El Sherbiny, S.A., Tony, M.A.: Synthesis, characterization and potential application of magnetized nanoparticles for photocatalysis of levafix ca reactive azo-dye in aqueous effluent (2021)
45. Soares, E.T.; Lansarin, M.A.; Moro, C.C.: A study of process variables for the photocatalytic degradation of rhodamine b. Braz. J. Chem. Eng. **24**(1), 29–36 (2007)
46. Gogate, P.R.; Pandit, A.B.: A review of imperative technologies for wastewater treatment i: oxidation technologies at ambient conditions. Adv. Environ. Res. **8**(3–4), 501–551 (2004)
47. Tony, M.A.; Lin, L.S.: Attenuation of organics contamination in polymers processing effluent using iron-based sludge: process optimization and oxidation mechanism. Environ. Technol. (2020). https://doi.org/10.1080/09593330.2020.1803417
48. Oliveira, C.; Gruskevica, K.; Juhna, T., et al.: Drink. Water Eng. Sci. **7**(1), 11 (2014)
49. Thabet, R.H.; Fouad, M.K.; El Sherbiny, S.A.; Tony, M.A.: Solar assisted green photocatalysis for deducing carbamate insecticide from agriculture stream into water reclaiming opportunity. Int. J. Environ. Anal. Chem. (2022). https://doi.org/10.1080/03067319.2022.2027930
50. Raut-Jadhav, S.; Pinjari, D.V.; Saini, D.R.; Sonawane, S.H.; Pandit, A.B.: Intensification of degradation of methomyl (carbamate group pesticide) by using the combination of ultrasonic cavitation and process intensifying additives. Ultrason. Sonochem. **31**, 135–142 (2016)
51. Tony, M.A.: Zeolite-based adsorbent from alum sludge residue for textile wastewater treatment. Int. J. Environ. Sci. Technol. (2020). https://doi.org/10.1007/s13762-020-02646-8
52. Ahmadi, M.; et al.: A novel catalytic process for degradation of bisphenol A from aqueous solutions: a synergistic effect of nano-Fe_3O_4@Alg-Fe on O_3/H_2O_2. Process Saf. Environ. Prot. **104**, 413–421 (2016)
53. Argun, M.E.; Karatas, M.: Application of fenton process for decolorization of reactive black 5 from synthetic wastewater: kinetics and thermodynamics. Environ. Prog. Sustain. Energy **30**(4), 540–548 (2011)
54. Pourali, P.; Behzad, M.; Arfaeinia, H.; Ahmadfazeli, A.; Afshin, S.; Poureshgh, Y.; Rashtbari, Y.: Removal of acid blue 113 from aqueous solutions using low-cost adsorbent: adsorption isotherms, thermodynamics, kinetics and regeneration studies. Sep. Sci. Technol. 1–13 (2021).
55. Ahmadi, M.; Behin, J.; Mahnam, A.R.: Kinetics and thermodynamics of peroxydisulfate oxidation of reactive yellow 84. J. Saudi Chem. Soc. **20**(6), 644–650 (2016)
56. SAS: STAT: User's Guide. SAS Institute Inc., Cary, NC (1990)
57. Tony, M.A.: Central composite design optimization of bismarck dye oxidation from textile effluent with Fenton's reagent. Appl. Water Sci. **10**(5), 1–9 (2020)